DVB-H Field Measurement and Data Analysis Method

Jyrki T.J. Penttinen
Member, IEEE
jyrki.penttinen@nsn.com

Abstract

The field measurement equipment that provides reliable results is essential in the quality verification of DVB-H (Digital Video Broadcasting, Hand held) networks. In addition, sufficiently in-depth analysis of the post-processed data is important. This paper presents a method to collect and analyze key performance indicators of the DVB-H radio interface by using a mobile device as a measurement and data collection unit.

Index Terms—*DVB-H, mobile broadcast, radio network planning, network performance evaluation.*

1. Introduction

The verification of the DVB-H quality of service level can be done by carrying out field measurements within the coverage area. Correct way to obtain the most relevant measurement data, as well as the right interpretation of it, are fundamental for the detailed network planning and optimization as described in the paper [1] (ICDT 2008).

During the normal operation of the DVB-H network, there are only few possibilities to carry out long-lasting and in-depth measurements. A simple and fast field measurement method based on mobile DVB-H receiver provides thus added value for the operator. The mobile equipment is easy to carry both in outdoor and indoor environment, and it stores sufficiently detailed performance data for the post-processing.

The measurements are required for the network performance revisions and for the indication of potential problems. As an example, the transmitter site antenna element might move due to the loose mounting, which results outages in the designed coverage area. The antenna feeder might still remain connected correctly, keeping the reflected power in acceptable level. As there are no alarms triggered in this type of instance, and as the basic DVB-H is a broadcast system without uplink and its related monitoring / alarming system, the most efficient way to verify this kind of fails is to carry out field tests.

This paper is an extension to the publication [1], presenting a method to post-process the field test data collected with DVB-H mobile terminal. The method can be considered as an addition to the usual network performance testing carried out by the operator and is suitable for the fast revisions of the radio quality levels and possible network faults.

The results presented in this paper are meant as examples and for clarifying the analysis methodology. The more detailed guidelines and examples of the related results can be found e.g. in [2, 3, 4, 5, 6]. The data was collected with a commercial DVB-H hand-held terminal capable of measuring and storing the radio link related data. In this specific case, a Nokia N-92 terminal was used with a field test program. The program has been developed by Nokia for displaying and storing the most relevant DVB-H radio performance indicators.

2. Coding of DVB-H

In order to carry the DVB-H IP datagrams of the MPEG-2 Transport Stream (TS), a Multi Protocol Encapsulator (MPE) is defined for DVB. Each IP datagram is encapsulated into single MPE section. Elementary Stream (ES) takes care of the transporting of these MPE sections. Elementary Stream is thus a stream of packets belonging to the MPEG-2 Transport Stream and with a respective program identifier (PID). The MPE section consists of 12 byte header, 4 byte CRC-32 (Cyclic Redundancy Check), as well as a tail and payload length as described in [2, 7].

The main idea of MPE-FEC is to protect the IP datagrams of the time sliced burst with an additional link layer Reed-Solomon (RS) parity data. The RS data is encapsulated into the same MPE-FEC sections of the burst with the actual data. The RS part of the burst belongs into the same elementary stream (MPE-FEC section), but they have different table identifications.

The benefit of this solution is that the receiver can distinguish between these sections, and if the terminal does not have the capability to use the DVB-H specific MPE-FEC, it can anyway decode the bursts although with lower quality when it experiences difficult radio conditions, according to [7, 8, 9, 10].

The part of the MPE-FEC frame that includes the IP datagrams is called application data table (ADT). ADT has a total of 191 columns. In case the IP datagrams do not fill completely the ADT field, the remaining part is padded with zeros. The division between ADT and RS table is shown in Figure 1.

In DVB-H system, the number of the RS rows can be selected from the values of 256, 512, 768 and 1024. The amount of the rows is indicated in the signaling via the Service Information (SI). RS data has a total of 64 columns.

For each row, the 191 IP datagram bytes are used for calculating 64 parity bytes of RS rows. Also in this case, if the row is not filled completely, padding is used. The result is a relative deep interleaving as the application data is distributed for the whole bust.

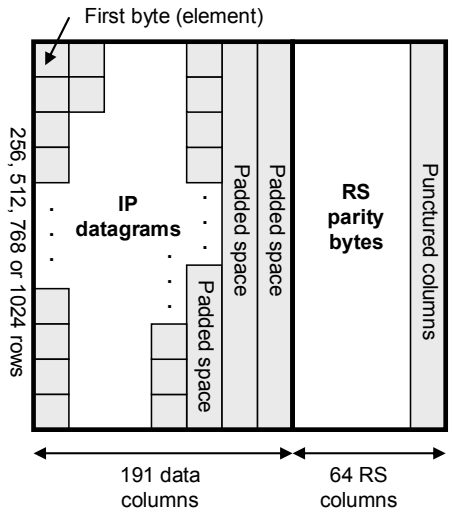

Figure 1. The MPE-FEC frame consists of application data table for IP datagrams and Reed-Solomon data table for RS parity bytes.

The error correction of DVB-H is carried out with the widely used Reed-Solomon coding. The Reed-Solomon code is based on the polynomial correction method. The polynomial is encoded for the transmission over the air interface. If the data is corrupted during the transmission, the receiving end can calculate the expected values of the data within the certain limits that depends on the settings.

The RS data of DVB-H is sent in encoded blocks with the total number of m-bit symbols in the encoded block is $n=2^m-1$. With 8-bit symbols the amount of symbols per block is $n= 2^8-1 = 255$. This is thus the total size of the DVB-H frame.

The actual user data inside of the frame is defined as a parameter with a value k, which is the number of data symbols per block. Normal value of k is 223 and the parity symbol is 32 (with 8 bits per symbol). The universal format of presenting these values is $(n,k) = (255,223)$. In this case, the code is capable of correcting up to 16 symbol errors per block.

RS can correct errors depending on the redundancy of the block. For the erroneous symbols which location is not known in advance, the RS code is capable of correcting up to $(n-k)/2$ symbols that contains errors. This means that RS can correct half as many errors as the amount of redundancy symbols is added in the block.

If the location of errors is known (i.e. in case of erasures) then RS can correct twice as many erasures as errors. If N_{err} is the number of errors and N_{ers} the number of erasures in the block, the combination of error correction capability is obtained according to the formula $2N_{err} + N_{ers} < n$.

The characteristic of RS error correction is thus well suited to the environment with high probability of errors occurring in bursts, like in DVB-H radio interface. This is because it does not matter how many bits in the symbol are erroneous – if multiple errors occur in byte, it is considered as a single error.

It is possible to use also other block sizes. The shortening can be done by padding the remaining (empty) part of the block (bytes). These padded bytes are not transmitted, but the receiving end fills in automatically the empty space.

FEC (Forward Error Correction) is widely used in telecommunication systems in order to control the errors. In this method, the transmitting party adds redundant data to the message. On the other side, the receiving end can detect and correct the errors accordingly without the need to acknowledge the data correction. The method is thus suitable for especially uni-directional broadcast networks.

FEC consists of block coding and convolutional coding. RS is an example of the block coding, where blocks or packets of bits (symbols) are of fixed size whereas convolutional coding is based on bit or symbol lengths.

In practice, the block and convolutional codes are combined in concatenated coding schemes; the convolutional coding has the major role whereas the block code like RS cleans the errors after the convolutional coding has taken place. In mobile communica-

tions, the convolutional codes are mostly decoded with the Viterbi algorithm. It is an error-correction scheme especially suitable for noisy digital communication links.

The MPE-FEC has been designed taking into account the backwards compatibility. The DVB-T demodulation procedure contains error correction so both DVB-T and DVB-H utilizes it for the basic coding with Viterbi and Reed-Solomon decoding, whereas DVB-H can use also a combination of Viterbi, Reed-Solomon and additional MPE-FEC to improve the *C*/*N* and Doppler performance [7]. The detection of the presence of MPE-FEC is done based on the single demodulated TS packet, as its header contains the error flag. MPE-FEC adds the performance in moving environment as it uses so called virtual interleaving over several basic FEC sections.

In this study, the bit rates before and after the Viterbi as well as the frame error rates of DVB-H MPE-FEC and DVB-T specific FEC were observed by collecting and analyzing data in radio interface. The measurement principles of WingTV guidelines [2] were taken into consideration in the selection (limiting) of the parameter values.

The guideline defines the MFER (MPE Frame Error Ratio) as a ratio of the number of residual erroneous frames that can not be recovered to the total number of the received frames:

$$MFER(\%) = 100\frac{residual\_erroneous\_frames}{received\_frames}$$

There are possibilities to obtain the MFER value by observing the frames during certain time (e.g. 20 seconds), or as proposed by DVB, at least 100 frames should be collected in order to calculate the MFER with sufficient statistical reliability.

The measurement principles of WingTV were used as a basis in the study by collecting 25 minutes of field data during a drive test with varying speeds, and the data was later post-processed in order to obtain the more specific relation between the FER, MFER and received power level categories. Although WingTV does not recommend the use of QEF as a criterion, also the bit errors were analyzed by utilizing the same principles for the comparison purposes.

3. Test setup

A test setup with a functional DVB-H transmitter site was utilized in order to investigate the presented field test methodology with respective post-processing and analysis. The site antenna safety distance zone was estimated by applying [11]. The investigated area represents relatively open sub-urban environment as shown in Figure 2. There are mainly relatively small trees, residential areas and highways in the investigated area with nearly-LOS in major part of the investigated area.

Figure 2. The environment in main lobe of the transmitter antenna.

The methodology was verified by carrying out various field tests mostly in vehicle. There was also static and dynamic pedestrian type of measurements included in the test cases in order to verify the usability of the equipment and methodology for the analysis.

The DVB-H test network consisted of a single 200 watt DVB-H transmitter and a basic DVB-H core network. The source data was delivered to the radio interface by capturing real-time television program. The program was converted to DVB-H IP data stream with standard DVB-H encoders. There was a set of 3 DVB-H channels defined in the same radio frequency, with audio / video bit rates of 128, 256 and 384 kb/s. The number of FEC rows was selected as 256 for MPE-FEC rate of 1/2, and 512 for MPE-FEC rate of 2/3. The audio part of the channel was coded with AAC using a total of 64 kb/s for stereophonic sound. The bandwidth was 6 MHz in 701 MHz frequency.

The antenna system consisted of directional antenna panel array with 2 elements as shown in Figure 3. Each element produces 65 degrees of horizontal beam width and provides a gain of +13.1 dBi.

Figure 3. The antenna system setup.

The vertical beam width of the single antenna element was 27 degrees, which was narrowed by locating two antennas on top of each others via a power splitter. Taking into account the loss of cabling, jumpers, connectors, power splitter and transmitter filter, the radiating power was estimated to be +62.0 dBm (EIRP) in the main lobe.

The transmitter antenna system was installed on a rooftop with 30 meters of height from the ground. The environment consisted of sub-urban and residential types with LOS (line-of-sight) or nearly LOS in major part of the test route, excluding the back lobe direction of the site which was non-LOS due to the shadowing of the site building. Each test route consisted of two rounds in the main lobe of the antenna with a minimum received power level of about -90 dBm. The maximum distance between the antenna system and terminals was about 6.4 km during the drive tests.

The terminals were kept in the same position inside the vehicle without external antenna, and the results of each test case were saved in separate text files. The terminal setup is shown in Figure 4. The external antenna was not used because the aim was to revise the quality that the end-user experiences in normal conditions inside the moving vehicle. On the other hand, the test cases were not designed for certain coverage area, but the aim was to classify the performance indicators in function of the received power levels. It does not matter thus if the received power level is interpreted via external or internal antenna.

Figure 4. The terminal measurement setup.

If the relevant data can be measured from the radio interface and stored in text format, the method presented in this paper is independent of the terminal type. It is important to notice, though, that the characteristics of the terminal affects on the analysis, i.e. the terminal noise factor and the antenna gain (which is normally negative in case of small DVB-H terminals) should be taken into account accordingly. On the other hand, unlike with the advanced field measurement equipment, the method gives a good idea about the quality that the DVB-H users observe in real life as the terminal type with its limitations is the same as used in commercial networks.

There were a total of 3 terminals used in each test case for capturing the radio signal simultaneously. Multiple receptions provide respectively more data to be collected at the same time, which increases the statistical reliability of the measurements. It also makes possible the comparison of the differences between the terminal performances.

4. Terminal measurement principles

The DVB-H parameter set was adjusted according to each test case. The cases included the variation of the code rate (CR) with the values of 1/2 and 2/3, MPE-FEC rate with the values of 1/2 and 2/3 and interleaving size FFT with the values of 2k, 4k, 8k, in accordance with the Wing TV principles described in [3], [4], [5] and [6]. The guard interval (GI) was fixed to 1/4 in each case. The parameter set was tuned for each case, and the audio / video stream was received with all the terminals by driving the test route two consecutive times per each parameter setting.

The needed input for the field test is the “on” and “off” time of the time sliced burst, PID (Packet Identifier) of the investigated burst, the number of FEC rows and the radio parameter values (frequency, modulation, code rate and bandwidth). The terminal stores the measurement results to a log file after the end of each burst until the field test execution is terminated.

According to the DVB-H implementation guide-lines [2], the target quality of service is the following:

- For the bit error rate after Viterbi (BA), the reception should comply at least DVB-H specific QEF (quasi error free) point $2 \cdot 10^{-4}$.
- The frame error rate should be less than 5%. In case of FER, i.e. DVB-T, this criterion is called FER5, and for the DVB-H specific MPE-FEC, its name is MFER5.

The field test software of N-92 is capable of collecting the RSSI (received power levels in dBm), FER (Frame Error Rate) and MFER (MPE Frame Error Rate, i.e. FER after MPE-FEC correction) values. In addition, there is possibility to collect information about the packet errors.

Figure 5 shows a high-level block diagram of the DVB-H receiver [2]. The reception of the Transport Stream (TS) is compatible with DVB-T system, and the demodulation is thus done with the same principles also in DVB-H. The additional DVB-H specific functionality consists of Time Sliced burst handling, MPE-FEC module and the DVB-H de-encapsulation.

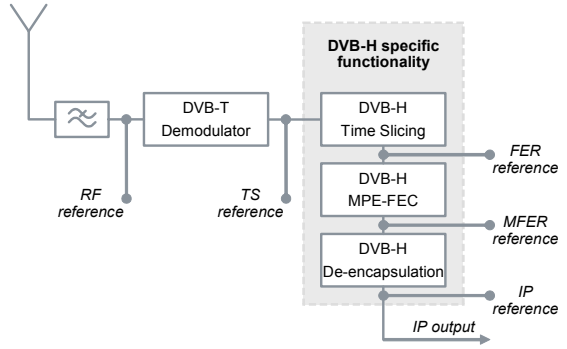

Figure 5. A principle of the reference DVB-H terminal.

As can be seen from Figure 5, the FER information, i.e. frame errors before MPE-FEC specific analysis, is obtained after the Time Slicing process, and the MFER is obtained after the MPE-FEC module. If the data after MPE-FEC is free of errors, the respective data frame is de-encapsulated correctly and the IP output stream can be observed without disturbances.

The measurement point for the received power level is found after the antenna element and the optional GSM interference filter. In addition, there might be optional external antenna connector implemented in the terminal before the RF reference point. The presence of the filter and antenna connector has thus frequency-dependent loss effect on the measured received power level in the RF point.

Figure 6 shows an example of the measurement data file. The example shows 4 consecutive test results. Each measurement field contains information about the occurred frame error (FER), frame error after MPE-FEC correction (MFER), bit error rate before Viterbi (BB) and after Viterbi (BA), packet errors (PA) and received power level (RSSI) in dBm. In this case, there was a frame error in the reception of the first measurement sample because the value of FER was "1". The FER value is either "0" for non-erroneous or "1" for erroneous frame. The MPE-FEC procedure could still recover the error in this case, because the MFER parameter is showing a value of "0". The second sample shows that there were no frame errors before or after the MPE-FEC. The third sample shows again frame error that could be corrected with MPE-FEC. The fourth sample shows an error that could not be corrected any more with MPE-FEC. In the latter case, the bit error information could not be calculated either. It seems that in this specific case, the RSSI value of about -87 dBm to -89 dBm has been the limit for the correct reception of the frames with MPE-FEC.

```
 FER:  1 MFER:  0
BB:2.5e-02 BA:1.2e-03
PE:  75
RSSI: -89
 FER:  0 MFER:  0
BB:4.5e-02 BA:1.7e-03
PE:  25
RSSI: -89
 FER:  1 MFER:  0
BB:3.6e-02 BA:8.2e-04
PE:   7
RSSI: -88
 FER:  1 MFER:  1
BB:0.0e+00 BA:0.0e+00
PE:   0
RSSI: -87
```

Figure 6. Example of the measured objects with four consecutive results for FER, MFER, BB, BA, PE and RSSI.

The plain measurement data has to be post-processed in order to analyze the breaking points for the edge of the performance. Microsoft Excel functionality was utilized in order to arrange the data in function of the received power levels.

According to the first sample of Figure 6, the bit error level before Viterbi (BB) was close to the QEF point, i.e. $2.5 \cdot 10^{-2}$. The bit error level after the Viterbi (BA) was $1.2 \cdot 10^{-3}$ which is already better than the QEF point for the acceptable reception. The bit error rate had been thus low enough for the correct reception of the signal. In this example, the amount of packet errors (PE) was between 7 and 75, and the averaged received power level was measured and averaged to -87…-89 dBm. It is worth noting that the RSSI resolution is 1 dB for single measurement event in the used version of the field test software.

Figure 7 shows the measured RSSI values during the complete test route. There were two rounds done during each test. The back lobe area of the test route can be seen in the middle of Figure, with fast momentarily drop of received power level. The received power level was about -50 dBm close to the site, and about -90 dBm in the cell edge. The duration of the single test route was approximately 25 minutes, and the total length of the route was 22.4 km.

The maximum speed during the test route was about 90 km/h, and the average speed was measured to 50 km/h (excluding the full stop periods). The speed is sufficient for identifying the effect of the MPE-FEC.

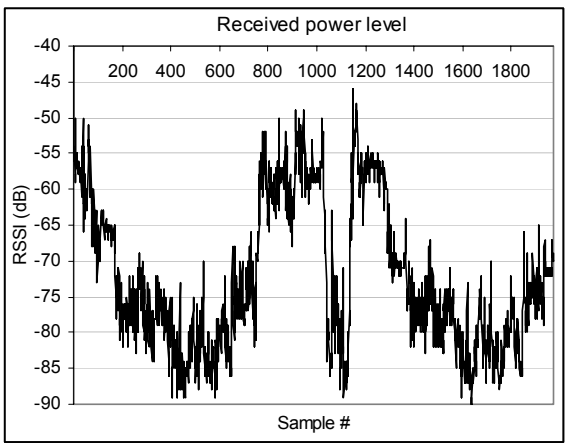

Figure 7. The RSSI values measured during the test route.

Figures 8 and 9 present the estimated coverage area for QPSK and 16-QAM cases with the code rate of 1/2 and MPE-FEC rate of 3/4. The Okumura-Hata based propagation model [10] was used with a digital map that contains the elevation data and cluster type information. The minimum received outdoor power level limit for QPSK was estimated as -84 dBm and for 16-QAM as -78 dBm.

The 80 % area location probability criterion was used in these coverage plots. The grid size is 1.6 km. (Background map source: Google Map).

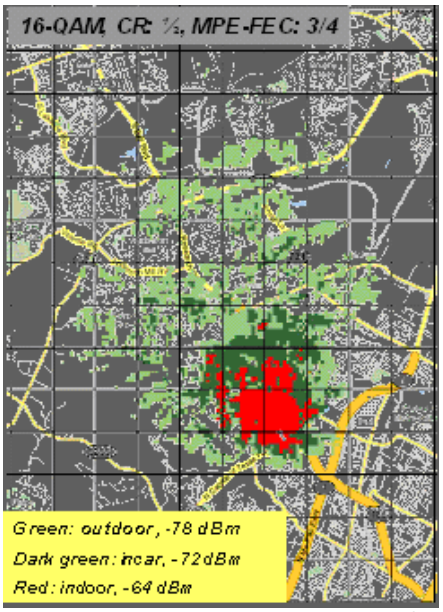

Figure 8. The predicted coverage area for 16-QAM. The raster shown in the map is 1.6 km. The main lobe and the test route is to north-west direction form the site.

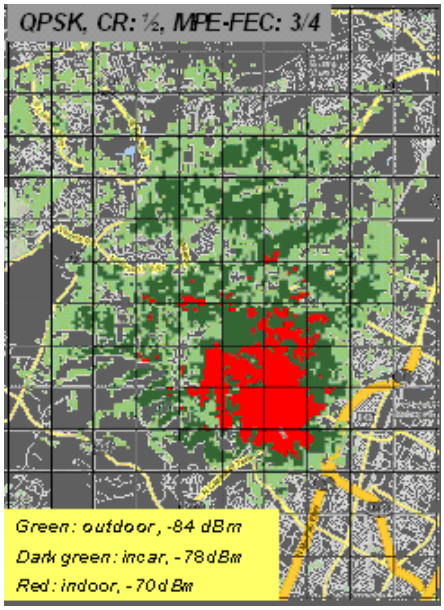

Figure 9. The predicted coverage area for QPSK, with the raster size of 1.6 km.

Based on the coverage plots, the test route was selected accordingly. The coverage plots correlated roughly with the drive tests, although the in-depth location-dependent signal level measurements were not carried out during this specific study.

5. Method for the analysis

The collected data was processed accordingly in order to obtain the breaking points, i.e. the QEF of $2 \cdot 10^{-4}$ and FER / MFER of 5% in function of the RSSI values for each test case. The processing was carried out by arranging the occurred events per RSSI value. For the BB and BA, the values were averaged per RSSI resolution of 1 dB. For the FER and MFER, the values represent the percentage of the erroneous frames compared to the total frame count per each individual RSSI value (with the resolution of 1 dB).

Figure 10 shows an example of the processed data for the bit error rate before and after the Viterbi for 16-QAM, CR 2/3, MPE-FEC 2/3 and FFT 2k. The results represent the situation over the whole test route in location-independent way, i.e. the results show the collected and averaged BB and BA values that have occurred related to each RSSI value in varying radio conditions.

As can be noted in this specific example, the bit error rate before Viterbi does not comply with the QEF criteria of $2 \cdot 10^{-4}$ even in relatively good radio conditions, whereas the Viterbi clearly enhances the performance. The resulting breaking point for the QEF

with Viterbi can be found around -78 dBm of RSSI in this specific case.

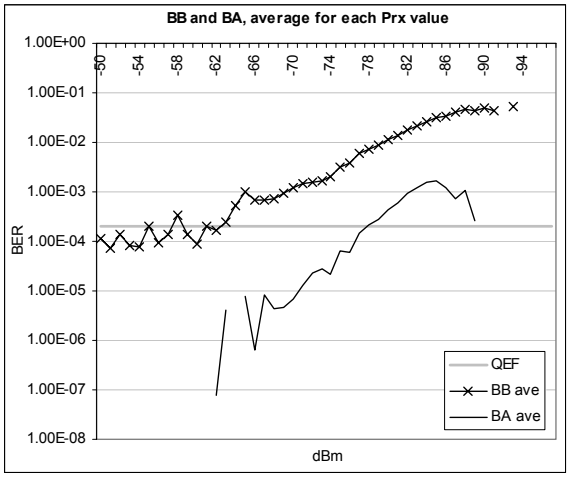

Figure 10. Post-processed data for the bit error rate before and after the Viterbi presented in logarithmic scale.

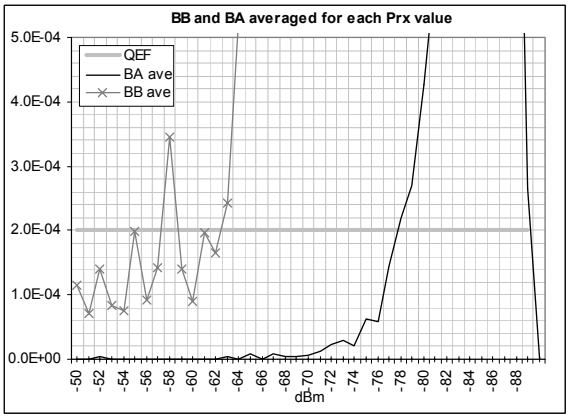

Figure 11. Processed data for the bit error rate before and after the Viterbi with an amplified view around the QEF point in linear scale.

For the frame error rate, the similar analysis yields an example that can be observed in Figure 12. Figure shows the occurred frame error counts (FER and MFER) as well as the amount of error-free events analyzed separately for each RSSI value. In this format, Figure 12 shows the amount of occurred samples in function of RSSI in 1 dB raster arranged to error free counts ("FER0, MFER0"), to counts that had error but could be corrected with MPE-FEC ("FER1, MFER0"), and to counts that were erroneous even after MPE-FEC ("FER1, MFER1").

It can be noted that the amount of the occurred events is relatively low in the best field strength cases and does not necessarily provide with sufficient statistical reliability in that range of RSSI values. Nevertheless, as the idea was to observe the performance especially in the limits of the coverage area, it is sufficient to collect reliable data around the critical RSSI value ranges.

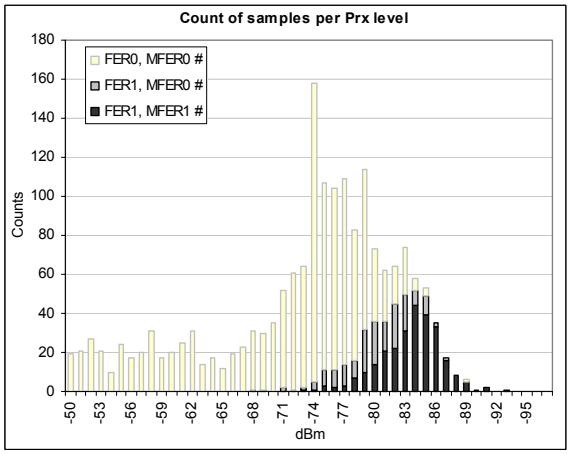

Figure 12. Example of the analyzed FER and MFER levels of the signal.

In this type of analysis, the data begins to be statistically sufficiently reliable when several tens of occasions per RSSI value are obtained, preferably around 100 samples as stated in [3]. In practice, though, the problem arises from the available time for the measurements, i.e. in order to collect about 100 samples per RSSI value in large scale it might take more than one hour to complete a single test case. There were a total of 32 test drive rounds carried out, 25 minutes each. In this case, the post-processing and analysis was limited to 2 terminals though due to the extensive amount of data.

The corresponding amount of total samples was normalized, i.e. scaled to 0-100% separately for each RSSI value. An example of this is shown in Figures 13 and 14.

By presenting the results in this way, the percentage of FER and MFER per RSSI and thus the breaking point of FER / MFER can be obtained graphically.

The 5% FER and MFER levels, i.e. FER5 and MFER5, can be obtained graphically for each case observing the breaking point for the respective curves. The corresponding MPE-FEC gain can be interpreted by investigating the difference between FER5 and MFER5 values (in dB). The graphics shows the observation point directly along the 5% error line. The parameter values of the following examples are still 16-QAM, CR 2/3, MPE-FEC 2/3 and FFT 2k.

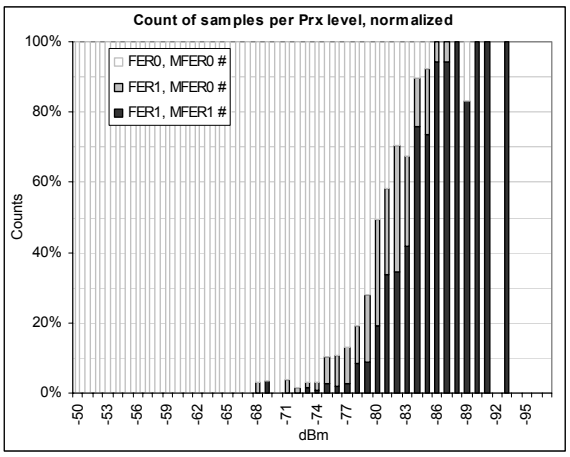

Figure 13. The post-processed data can be presented in graphical format with FER and MFER percentages for each RSSI value.

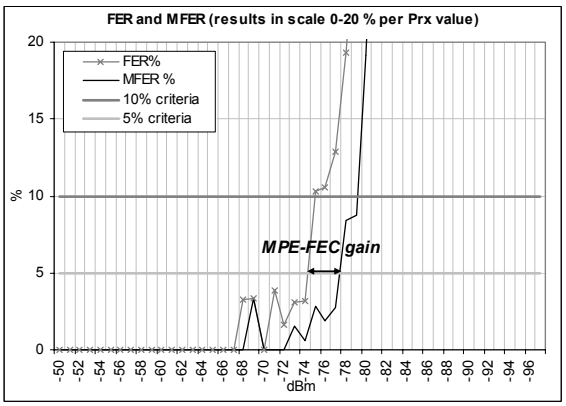

Figure 14. An amplified view to FER5 and MFER5 criteria shows the respective RSSI breaking points.

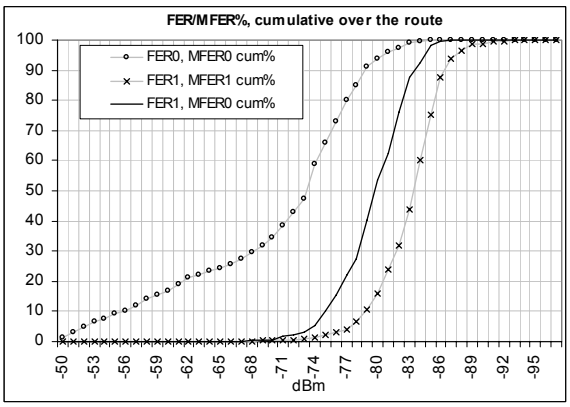

Figure 15. The processed data can also be presented in cumulative format over the whole route. This presentation gives a rough estimate about the RSSI range of the correction.

As additional information about the FEC and MPE-FEC performance in the whole scale of 0-100%, the cumulative presentation can be observed as shown in Figure 15. This format gives indication about the RSSI range where the MPE-FEC starts correcting.

The results presented in this case can be post-processed further in order to fragment the test routes into the more specific area and radio channel types. Figure 16 shows the segments during the test drive.

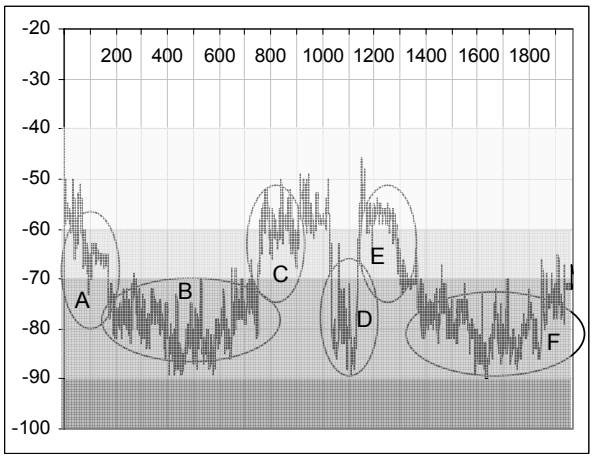

Figure 16. The segments of the test route.

Segments A and E represents the terminal moving away from the site in LOS within the main lobe of the antenna beam, with a maximum speed of about 70 km/hour and with a good field strength. Segments B and F represents the LOS or nearly LOS with the terminal moving with a maximum speed of 70-80 km/h, and the area represents the cell edge or near the cell edge, depending on the selected modes. Segment C represent the terminal moving towards the site with a maximum speed of 90 km/h, with a good field strength and LOS. Segment D represents the situation in back lobe of the antenna with N-LOS situation due to the shadowing of the site building, with the terminal speed varying between 0 and 80 km/h.

Having the segmentation done according to Figure 16, it can be seen that in the good field, as expected, the occurred FER and MFER instances are minimal and they do not affect on the reception of the DVB-H audio / video streams. Furthermore, the MPE-FEC does not bring enhancements for the performance within such a good field.

The most interesting parts of the segments are thus the ones that represents the situation nearer to the cell edge, both in main lobe (B and F) and in back lobe (D).

As an example, Figure 17 shows the analysis for the case QPSK, CR 2/3, MPE-FEC 1/2, and FFT 4k, indicating controlled behaviour of the FER and MFER until the breaking point, when the results from the segments B and F are combined and analyzed as a one complete block.

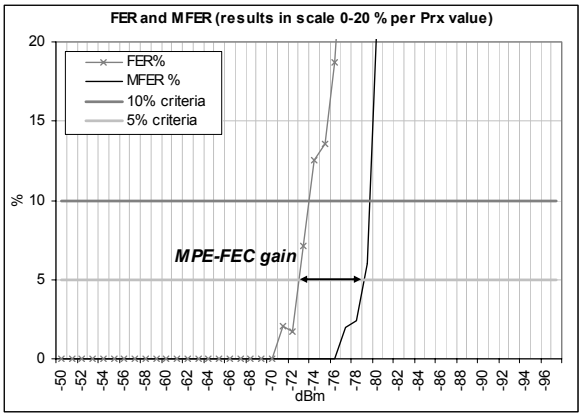

Figure 17. An example of the main lobe analysis with LOS. The curves are in general more controlled compared to the analysis of the whole route.

It is also interesting to investigate where in the RSSI scale the FER and MFER occasions have been occurred during these segments. Figure 18 shows the cumulative presentation of different FER and MFER occasions with above mentioned parameter values.

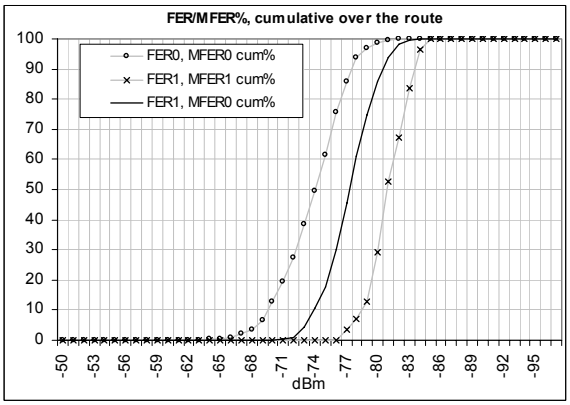

Figure 18. The cumulative presentation of FER and MFER gives a rough indication about the performance within the investigated area. Compared to Figure 15, the main lobe analysis produces clearer picture about single radio channel type.

It is worth noting, though, that this format gives only an indication about the RSSI range where the different modes of error correction tends to occur, i.e. the clean samples (FER0, MFER0), the successful MPE-FEC corrections (FER1, MFER0), and when the MPE-FEC is not able to correct the data (FER1, MFER1).

As a comparison, the N-LOS segment D yields Figures 19 and 20. The behaviour of the curves is not as clear as it is in main lobe. In addition to the attenuated N-LOS, the multi-path propagated signals are not strong in this area. It is though worth noting that the amount of the collected data is quite low, in order of 100-150 samples, which reduces considerably the reliability of the back lobe analysis.

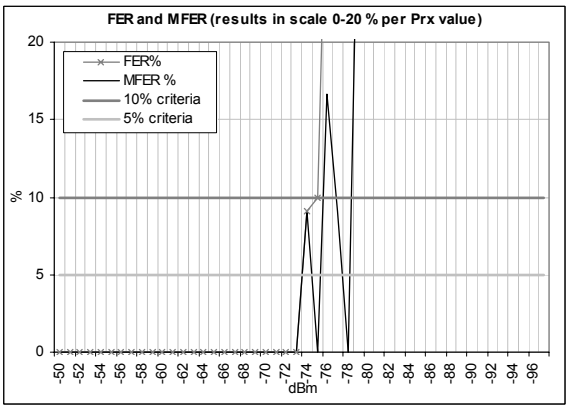

Figure 19. The back lobe analysis with N-LOS shows that the MPE-FEC is not able to correct the occurred frame error as efficiently as in main lobe with LOS. The respective segment has been selected from the same data file as shown in Figure 17 for the main lobe.

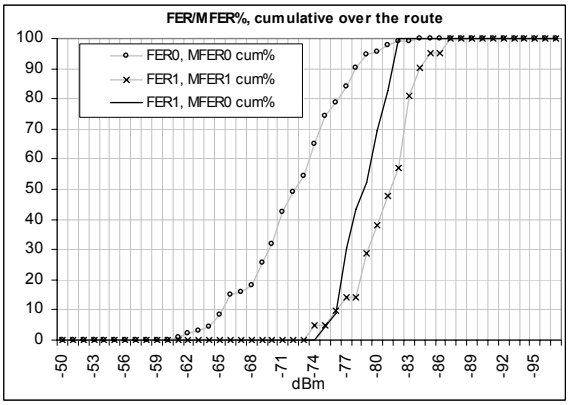

Figure 20. The cumulative presentation of back lobe analysis. It can be seen that the low amount of data affects clearly on the smoothness of the curves due to lack of data.

6. Terminal comparison

The terminal measures the received power level after the possible GSM interference suppression filter. There might also be external antenna connectors in either side of the filter. The terminal characteristics thus affects on the received power level interpretation. In order to obtain information about the possible differences of the terminal displays, separate comparison measurements were carried out.

There were a total of three terminals used during the testing. As the terminals were still prototypes, the calibration of the RSSI displays was not verified. This adds uncertainty factor to the test results.

Figure 21 shows a test case that was carried out in laboratory by keeping all the terminals in the same position and making slow-moving rounds within relatively good coverage area.

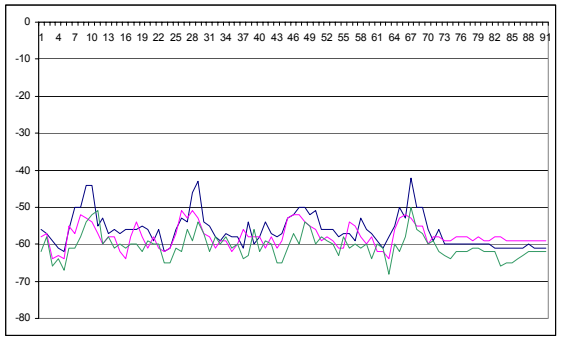

Figure 21. An example of the laboratory test case for the comparison of the RSSI displays of the terminals.

The systematic difference in RSSI displays can be noted, being about 2 dB between the extreme values. The same 2 dB difference between the terminals was noted in the field test analysis. The values obtained from the radio network tests cannot thus be considered accurate. Nevertheless, the idea of the testing was to investigate rather the methodology of the measurements than to obtain accurate values of the defined parameter settings.

In the in-depth analysis, in addition to the RSSI, also more specific differences between the terminals can be investigated. As Figures 22, 23 and 24 show, there is a systematic difference margin between the three utilized terminals as for the QEF, FER5 and MFER5. As a conclusion of Figures, in order to minimize the error margin that arises from the differences of the BER, FER and MFER interpretation of different terminals, it is important to calibrate the models accordingly.

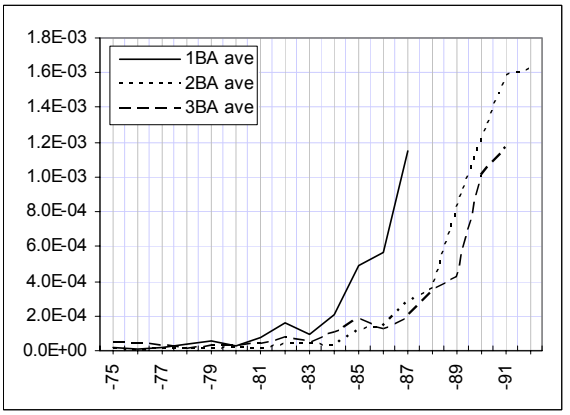

Figure 22. A comparison of 3 terminal models via BER measurement. It can be seen that two of the phones behave similarly whilst one is showing smaller bit error values.

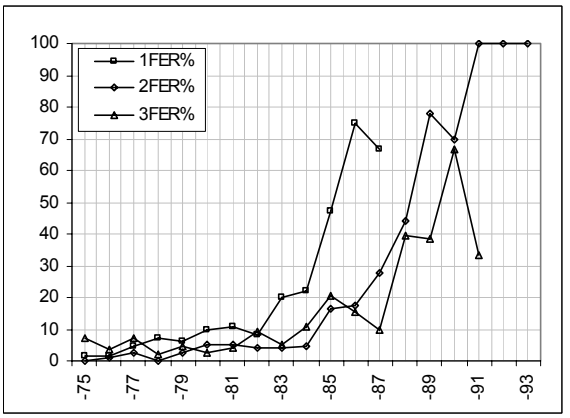

Figure 23. The systematic difference of the performance measurement values between the three terminals can be observed also via the FER curves.

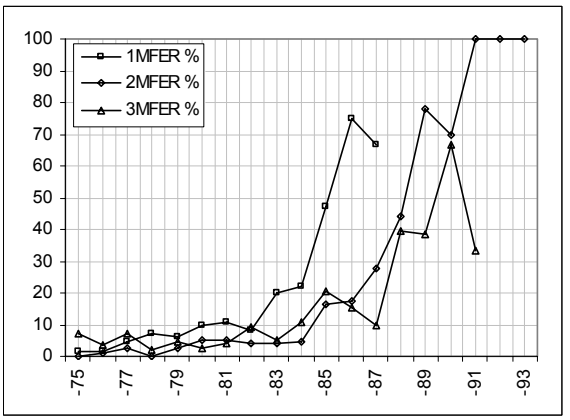

Figure 24. The differences of the terminals via the MFER analysis.

7. Building penetration loss

For the comparison purposes, there was also a set of test cases carried out in pedestrian environment with the same measurement methodology as described previously.

When designing the indoor coverage, the respective building loss should be taken into account. The loss depends on the building type and material. As an example, Figure 25 shows a relatively short measurement carried out in outdoor and indoor of a 10-floor hotel building within the coverage area of the investigated DVB-H network.

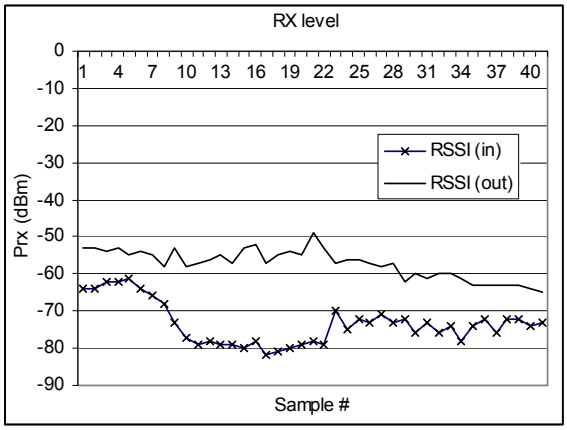

Figure 25. An example of short snap-shot type indoor and outdoor measurements carried out in the DVB-H trial network coverage area.

The building loss of Figure 25 can be obtained by calculating the difference of the received power values. The indoor average received power level is -73.4 dBm with a standard deviation of 5.7 dB. The outdoor values are -57.3 dBm and 3.9 dB, respectively. The building loss in this specific case is thus 16.1 dB. The value is logical as the building represents relatively heavy construction type, although the roof top was partially covered by large areas of class resulting relatively good signal propagation to interior of the building via the diffraction.

The test was repeated in selected spots inside and outside of the buildings, in variable field strengths both in main lobe and back lobe of the site antenna radiation pattern. As a general note, the static or low-speed pedestrian cases did not initiate the MPE-FEC functionality. Obviously more multi-path propagated signals and/or higher terminal speed would have been needed in order to "wake up" the MPE-FEC.

In the general case, the building loss should be estimated depending on the overall building type, height etc. in each environment type. In case of new areas, the best way for the estimation is to carry out sufficient amount of sample measurements for the most typical building types, although for the initial link budget estimations, the average of 12-16 dB could be a good starting point according to these tests.

8. Effects on the coverage estimation

Based on the measurement results, a tuned link budget can now be build up by using the essential radio parameters according to Figure 26.

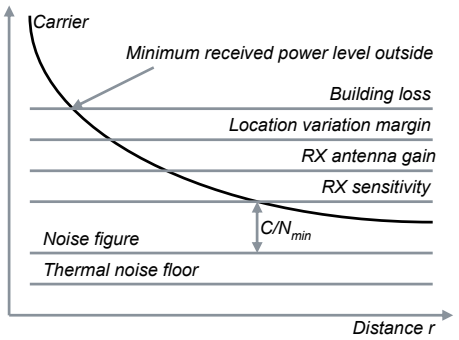

Figure 26. The main principle of the DVB-H link budget.

In order to estimate the useful cell radius of the DVB-H radio transmission, propagation prediction models can be used. One of the most used one in broadcast environment is the Okumura-Hata model, which is suitable as such for the macro cell type of environments [12]. The model functions sufficiently well in practice when the height of the transmitter site antenna is below 200 meters, and the frequency range is of 150-1500 MHz. The model is reliable for the cell ranges up to 20 km. The corrected Okumura-Hata prediction model for the distances over 20 km is defined in CCIR report 567-3. It is sufficient to estimate the cell radius for the high-power DVB-H transmitter sites with the radius up to 50 km. The most recent model that is especially suitable for the large variety of distances and transmitter antenna heights is ITU-R P.1546, which is based on the mapping of the pre-calculated curves. [13]

Based on the field test examples shown previously, the MPE-FEC gain can be included for the sensitivity Figure, compared to the DVB-T case which contains only FEC. The gain varies depending on the terminal speed and environment type, so the fine-tuning of the link budget should be considered depending on the local conditions.

9. Field test results

9.1. Complete route

As a result of the vehicle based field tests performed in this study, the following Tables 1-3 summarizes the RSSI thresholds for the QEF point of $2 \cdot 10^{-4}$ and FER / MFER of 5% criteria with different parameter values for the whole test route. In addition, the effect of MPE-FEC was obtained graphically for each parameter setting. The analysis was made for the post-processed data by observing the breaking points of BA, FER and MFER of the averaged values of 2 terminals (the other one resulting 2 dB lower RSSI). The guard interval (GI) was set to 1/4 in each case.

The MPE-FEC gain was obtained for each studied case. The effect seems to be lowest for the 64-QAM modulation, which might be an indication of too small amount of collected data in the relatively good field that this mode requires, although 64-QAM seems to be in general very sensible for errors.

It should be noted, though, that the terminals were not calibrated especially for this study. The RSSI display might thus differ from the real received power levels with roughly 1-2 decibels. The calibration should be done e.g. by examining first the level of the noise floor of the terminal and secondly examining the QEF point, i.e. investigating the signal level which is just sufficient to provide the correct receiving.

Table 1. The results for QPSK cases. The values represent the RSSI in dBm, except for the MPE-FEC gain, which is shown in dB.

FFT	8k	8k	4k	2k
CR	1/2	2/3	2/3	2/3
5%, MPE-FEC1/2	-88,1	-83,8	-78,4	-86,6
5%, FEC 1/2	-84,0	-77,3	-72,7	-81,4
MPE-FEC 1/2 gain	4,1	6,5	5,7	5,2
5%, MPE-FEC 2/3	-87,3	-83,0	-76,7	-84,4
5%, FEC 2/3	-83,3	-72,9	-73,5	-81,0
MPE-FEC 2/3 gain	4,0	10,1	3,2	3,4
BA QEF average:	-85,8	-81,7	-78,4	-84,9

Table 2. The results for 16-QAM cases.

FFT	8k	8k	4k	2k
CR	1/2	2/3	2/3	2/3
5%, MPE-FEC1/2	-77,6	-61,8	-77,4	-77,7
5%, FEC 1/2	-69,8	-61,6	-74,2	-73,4
MPE-FEC 1/2 gain	7,8	0,3	3,7	4,3
5%, MPE-FEC 2/3	-77,0	-63,5	-75,5	-77,0
5%, FEC 2/3	-72,1	-59,0	-71,0	-74,7
MPE-FEC 2/3 gain	4,9	4,5	4,5	2,3
BA QEF average:	-78,3	-73,7	-77,2	-77,4

Table 3. The results for 64-QAM cases.

FFT	8k	8k	4k	2k
CR	1/2	2/3	2/3	2/3
5%, MPE-FEC1/2	-59,9	-51,6	-65,0	-67,3
5%, FEC 1/2	-59,7	-51,6	-57,5	-65,2
MPE-FEC 1/2 gain	0,2	0,1	7,5	2,1
5%, MPE-FEC 2/3	-61,0	-51,3	-59,5	-68,1
5%, FEC 2/3	-60,3	-50,6	-54,5	-65,8
MPE-FEC 2/3 gain	0,7	0,7	5,0	2,4
BA QEF average:	-60,7	-53,0	-61,9	-68,3

As stated in [2], the moving channel produces fast variations already in TU6 channel type (typical urban 6 km/h) in the QEF criterion making the interpretation of the bit error rate before Viterbi very challenging. This also leads to the uncertainty of the correct calculation of the bit error rate after Viterbi. For the bit error rate before and after Viterbi, it is not thus necessarily clear how the terminal calculates the BB and BA values especially in the cell edge with high error rates. It has been also stated e.g. in [14] that QEF is not suitable for the instantaneous measurement due to the high variation that occurs in the mobile channel. This phenomena can be noted in the field test results as the breaking points of the QEF does not necessarily map to the corresponding FER / MFER criteria of 5% or near of it. It can thus be assumed that the most reliable results are obtained by observing the FER / MFER of the data, because their error detection is carried out after the whole demodulation and decoding process.

Furthermore, especially the frame error rate reflects the practical situation as the user interpretation of the quality of the audio / video contents depends directly on the amount of correctly received frames.

Nevertheless, the results correlate with the theory of different parameter settings, as well as with the MPE-FEC gain although it varies largely in the obtained results depending on the mode. As the test route contained different radio channel types (different vehicle speeds, LOS, near-LOS and non-LOS behind the building), the mix of the propagation types causes this effect on the results. In order to obtain the values nearer to the theoretical ones, it is important to carry out the test cases in separate, uniform areas as the radio channel type is considered, but on the other hand, these results represent the real situation in the investigated area with a practical mix of radio channel types.

9.2. Segmented route in main lobe

The following Tables 4 and 5 show the analysis for selected parameter settings of the terminal 1 (with 2 dB lower RSSI display compared to others) in order to present the principle of the segmented analysis in the

main lobe with around -70…-90 dBm of RSSI and the terminal speed of about 80 km/s. In case the breaking points could not be interpreted explicitly from the graphics, N/A was marked to Tables.

Table 4. The results for the QPSK cases in the main lobe. The channel type is nearly LOS and the terminal speed is 80 km/h.

FFT CR	8k 1/2	8k 2/3	4k 2/3	2k 2/3
5%, MPE-FEC1/2	-74.4	-84.7	-78.7	-85.3
5%, FEC 1/2	-74.3	-77.3	-72.5	-77.6
MPE-FEC 1/2 gain	0.1	7.4	6.2	7.7
5%, MPE-FEC 2/3	N/A	-82.7	-76.9	-83.3
5%, FEC 2/3	N/A	-76.1	-74.9	-79.2
MPE-FEC 2/3 gain	N/A	6.6	2.0	4.1
BA QEF average:	-84.3	-79.5	-75.7	-80.4

Table 5. The results of the setup for 16-QAM.

FFT CR	8k 1/2	8k 2/3	4k 2/3	2k 2/3
5%, MPE-FEC1/2	N/A	N/A	-76.4	-76.6
5%, FEC 1/2	N/A	N/A	-72.1	-75.5
MPE-FEC 1/2 gain	N/A	N/A	4.3	1.1
5%, MPE-FEC 2/3	-79.2	N/A	-75.3	-76.7
5%, FEC 2/3	-72.5	N/A	-72.5	-75-2
MPE-FEC 2/3 gain	6.7	N/A	2.8	1.5
BA QEF average:	-76.0	-69.5	-73.4	-76.4

It is now interesting to observe the behaviour of the FEC and MFEC values in this single radio channel type. Figures 27-28 summarise the performance of the investigated parameter set in the main lobe in the graphical format.

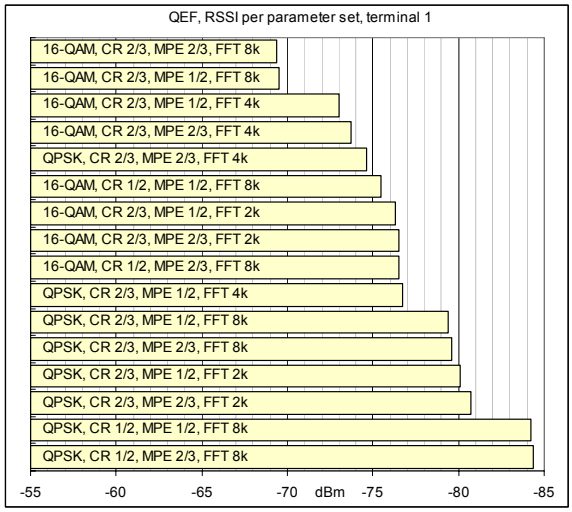

Figure 27. The summary of the QEF breaking points for the investigated parameter sets.

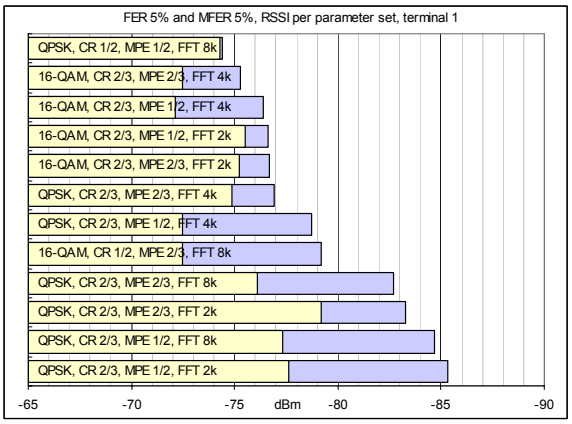

Figure 28. The summary of FER5 and MFER5 analysis.

It can be noted that the MPE-FEC functions more efficiently in this specific fragmented case, i.e. in the uniform radio channel of 80 km/h in cell edge area compared to the results obtained by analysing the whole test area with fixed radio channel types.

As a comparison, the difference of the QEF point and FER / MFER can now be obtained as shown in Figures 29 and 30.

In this case, it seems that the breaking point of QEF occurs somewhere between the FER5 and MFER5 values. As stated before, the QEF calculation is not necessarily as reliable as FER and MFER can show, but nevertheless, it is interesting to note that in this specific setup the QEF breaking point is within ±1.6 dB margin if we take simply the average of the FER and MFER values. QEF indicates thus the RSSI limits roughly in the same range as the FER and MFER does.

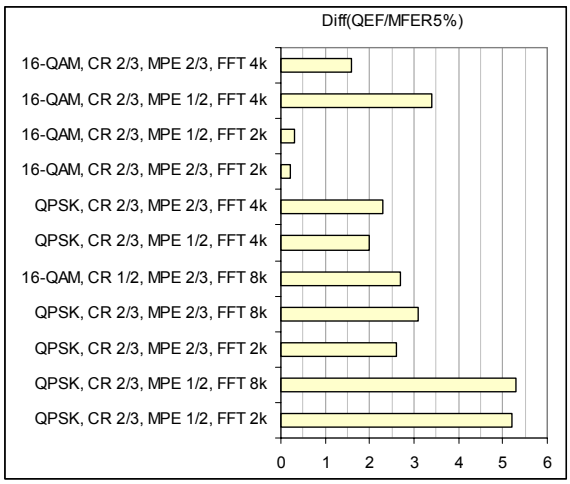

Figure 29. The difference of the QEF breaking points compared to the MFER5 results.

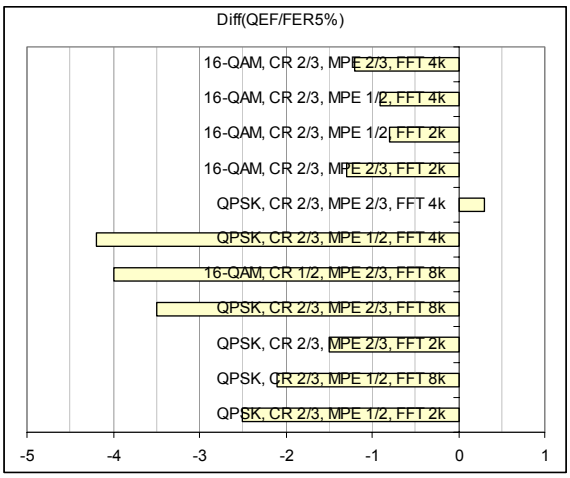

Figure 30. The difference of the QEF breaking points compared to the FER5 results.

10. Conclusions

The tests presented in this paper show that the realistic DVB-H measurement data can be collected with the terminals. The analysis showed correlation between the post-processed data and estimated coverage that was calculated and plotted separately with a network planning tool. The results correlate mostly with the theoretical DVB-H performance, although there was a set of uncertainty factors identified that affects on the accuracy of the results.

This study was meant to develop and verify the functionality of the methodology for measurements, post-processing and analysis, and as a secondary result, it also gave performance values for selected parameter set. The test environment consisted of multiple radio channel types, and the terminal displays were not calibrated specifically for these tests. An error of 1-2 decibels in RSSI values is thus expected.

The field test results show clearly the effect of the parameter values on radio performance in a typical sub-urban environment. Even if the hand-held terminal is not the most accurate device for the scientific purposes, it gives an overview about the general functioning and quality level of the network and the estimation of the effects of different network parameter settings.

The vehicle related test cases showed a logical functioning of MPE-FEC for different parameter settings. The results are in align with the theories especially when the analyzed data is limited to a single radio channel type in coverage edge of the main lobe with nearly LOS situation and with a vehicle speed of about 80 km/h. This case showed relatively significant effect of the MPE-FEC functionality giving a gain of up to 7 dB, which thus enhances the link budget and extends the coverage area compared to the basic FEC. On the other side, in the good field, the MPE-FEC is not needed as there are no frame errors present.

The whole test route can be analyzed also as one complete case, giving the overall information about the network performance in variable radio channels. It should be noted though that this case does not give comparable values for the performance measurements like the case is for the single radio channel.

The pedestrian test cases showed that the building loss can be obtained in easy way with the test setup. The analysis also showed that the MPE-FEC does not take place with such a low speeds even in low field strengths if there is lack of reflected multi-path propagated components. As the city center areas contains normally relatively good field and their main usage can be estimated to be pedestrian cases, the results indicates that the MPE-FEC setting could thus be relatively light in city areas, in order of 3/4 or 5/6, which gives still some MPE-FEC gain for sufficiently fast moving terminals, yet saving the capacity.

Regardless of the Excel sheet functionality that was developed for post-processing the data, there was a considerable amount of manual procedures in order to obtain the final results. As a possible future work item, basically all of the manual work can be automated by creating respective macro functionality for transferring the data from the terminal to the processing unit, to organize the data in function of the RSSI values, and to present the analysis in graphical and numerical format. Based on the methodology presented in this paper, the processing of the data is independent of the terminal type, but the special characteristics should be taken into account in the result tuning, as well as the proper calibration of the equipment. Furthermore, if the interface between the terminal and data processing unit supports proper protocols for fetching the data during the measurements, the post-processing and display can be performed in real time whilst carrying out the drive tests.

11. References

[1] Jyrki T.J. Penttinen. Field Measurement and Data Analysis Method for DVB-H Mobile Devices. The Third International Conference on Digital Telecommunications, 2008. IARIA, Published by the IEEE CS Press. 6 p.

[2] DVB-H Implementation Guidelines. Draft TR 102 377 V1.2.2 (2006-03). European Broadcasting Union. 108 p.

[3] Thibault Bouttevin (Editor). Wing TV. Services to Wireless, Integrated, Nomadic, GPRS-UMTS&TV handheld terminals. D8 – Wing TV Measurement Guidelines & Criteria. Project report. 45 p.

[4] Maite Aparicio (Editor). Wing TV. Services to Wireless, Integrated, Nomadic, GPRS-UMTS&TV handheld terminals. D6 – Wing TV Common field trials report. Project report, November 2006. 86 p.

[5] Maite Aparicio (Editor). Wing TV. Services to Wireless, Integrated, Nomadic, GPRS-UMTS&TV handheld terminals. D8 – Wing TV Country field trial report. Project report, November 2006. 258 p.

[6] Davide Milanesio (Editor). Wing TV. Services to Wireless Integrated, Nomadic, GPRS-UMTS&TV handheld terminals. D11 – WingTV Network Issues. Project report, May 2006. 140 p.

[7] Transmission System for Handheld Terminals (DVB-H). ETSI EN 302 304 V1.1.1 (2004-11). 14 p.

[8] Tero Jokela, Eero Lehtonen. Reed-Solomon Decoding Algorithms and Their Complexities at the DVB-H Link-Layer. IEEE 2007. 5 p.

[9] Teodor Iliev et al. Framing Structure, Channel Coding and Modulation for Digital Terrestrial Television. ETSI EN 300 744 V1.5.1 (2004-11). IEEE 2008. 5 p.

[10] Heidi Joki, Jarkko Paavola. A Novel Algorithm for Decapsulation and Decoding of DVB-H Link Layer Forward Error Correction. Department of Information Technology, University of Turku, 2006. 6 p.

[11] Limits of Human Exposure to Radiofrequency Electromagnetic Fields in the Frequency Range from 3 kHz to 399 GHz. Safety Code 6. Environmental Health Directorate, Health Protection Branch. Publication 99-EHD-237. Minister of Public Works and Government Services, Canada 1999. ISBN 0-662-28032-6. 40 p.

[12] Masaharu Hata. Empirical Formula for Propagation Loss in Land Mobile Radio Services. IEEE Transactions on Vehicular Technology, Vol. VT-29, No. 3, August 1980. 9 p.

[13] Recommendation ITU-R P.1546-3. Method for point-to-area predictions for terrestrial services in the frequency range 30 MHz to 3000 MHz. 2007. 57 p.

[14] Gerard Faria, Jukka A. Henriksson, Erik Stare, Pekka Talmola. DVB-H: Digital Broadcast Services to Handheld Devices. IEEE 2006. 16 p.

Biography

Mr. Jyrki T.J. Penttinen has worked in telecommunications area since 1994, for Telecom Finland and it's successors until 2004, and after that, for Nokia and Nokia Siemens Networks. He has carried out various international tasks, e.g. as a System Expert and Senior Network Architect in Finland, R&D Manager in Spain and Technical Manager in Mexico and USA. He currently holds a Senior Solutions Architect position in Madrid, Spain. His main activities have been related to mobile and DVB-H network design and optimization.

Mr. Penttinen obtained his M.Sc. (E.E.) and Licentiate of Technology (E.E.) degrees from Helsinki University of Technology (TKK) in 1994 and 1999, respectively. He has organized actively telecom courses and lectures. In addition, he has published various technical books and articles since 1996. His main books are "GSM-tekniikka" ("GSM Technology", published in Finnish, Helsinki, Finland, WSOY, 1999), "Wireless Data in GPRS" (published in Finnish and English, Helsinki, Finland, WSOY, 2002), and "Tietoliikennetekniikka" ("Telecommunications technology", published in Finnish, Helsinki, Finland, WSOY, 2006).